Can Age and Weight Predict Radial Carpal Bone Size in a Porcine Preclinical Model?

Quianna M. Vaughan, Amy Morton, Douglas C. Moore, Joseph J. Crisco

Department of Orthopaedics, Warren Alpert Medical School of Brown University and Rhode Island Hospital, Providence, RI

Click each section heading to see more

Introduction

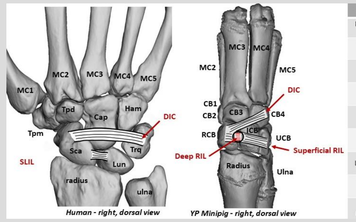

Human	YP Minipig
Metacarpals (MC1-5)	Metacarpals (MC2-4)
Trapezium (Tpm)	1st carpal bone (CB1)
Trapezoid (Tpd)	2nd carpal bone (CB2)
Capitate (Cap)	3rd carpal bone (CB3)
Hamate (Ham)	4th carpal bone (CB4)
Scaphoid (Sca)	Radial carpal bone (RCB)
Lunate (Lun)	Intermediate carpal bone (ICB)
Triquetrum (Trq)	Ulnar carpal bone (UCB)
Pisiform (not visible)	Accessory carpal bone (not visible)

Conclusion

Materials

Materialise Mimics

ShapeWorks

MATLAB®

Methodology

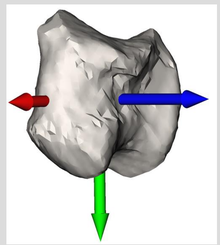

Results

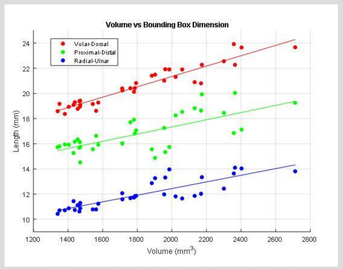

Can Age and Weight Predict Radial Carpal Bone Size in a Porcine Preclinical Model?

Quianna M. Vaughan, Amy Morton, Douglas C. Moore, Joseph J. Crisco

Department of Orthopaedics, Warren Alpert Medical School of Brown University and Rhode Island Hospital, Providence, RI

Introduction

- Wrist pathologies severely impact quality of life and surgical treatments typically affect the entire wrist
- Prosthetic replacement of individual carpal bones offers a therapeutic alternative, but to this point they have had limited success
- This overall goal of this study is to develop a radial carpal bone (RCB) replacement model in the Yucatan Minipig (YMP), chosen for its similarities to the human carpus
- The specific goal of this report is to:
  - Quantify YMP RCB size
  - Establish a method for estimating replacement RCB size based on age and weight, without the need for pre-op imaging

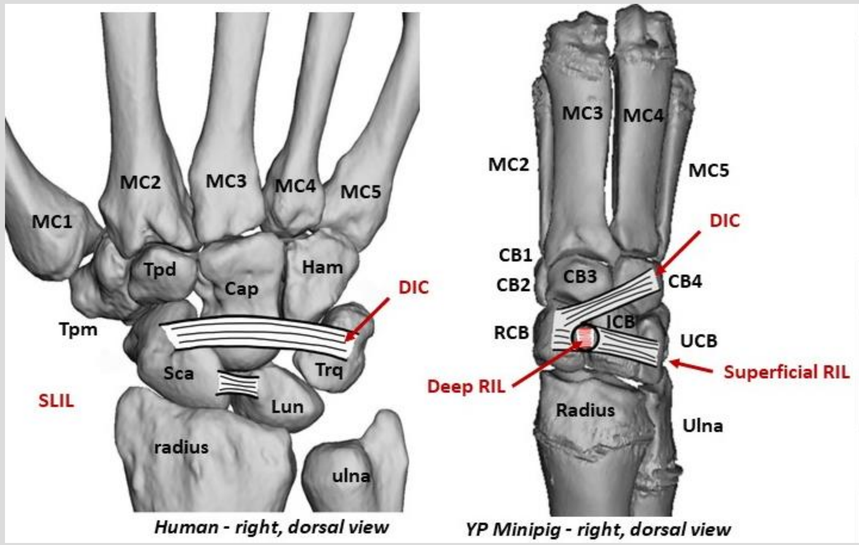

Human	YP Minipig
Metacarpals (MC1-5)	Metacarpals (MC2-4)
Trapezium (Tpm)	1st carpal bone (CB1)
Trapezoid (Tpd)	2nd carpal bone (CB2)
Capitate (Cap)	3rd carpal bone (CB3)
Hamate (Ham)	4th carpal bone (CB4)
Scaphoid (Sca)	Radial carpal bone (RCB)
Lunate (Lun)	Intermediate carpal bone (ICB)
Triquetrum (Trq)	Ulnar carpal bone (UCB)
Pisiform (*not visible*)	Accessory carpal bone (*not visible*)

Fig 1. Bone surface models of the human and YMP wrists from CT scans demonstrate similarities in bone morphology and ligamentous connections.

Can Age and Weight Predict Radial Carpal Bone Size in a Porcine Preclinical Model?

Quianna M. Vaughan, Amy Morton, Douglas C. Moore, Joseph J. Crisco

Department of Orthopaedics, Warren Alpert Medical School of Brown University and Rhode Island Hospital, Providence, RI

Materials

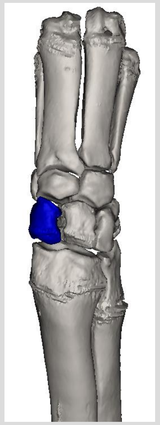

- 18 paired YMP forelimbs
  - 6 males, 12 females
  - Age: 25.1 ± 9.8 months
  - Weight: 62.6 ± 15.2 kg
- CT images of YMP forelimbs
  - 0.4 mm x 0.4 mm in-plane
  - 0.625 mm slice thickness
- MIMICS v22- segmentation to obtain 3D bone models
- MATLAB- bone size and regression models
- ShapeWorks Studio- statistical shape model (SSM)

Can Age and Weight Predict Radial Carpal Bone Size in a Porcine Preclinical Model?

Quianna M. Vaughan, Amy Morton, Douglas C. Moore, Joseph J. Crisco

Department of Orthopaedics, Warren Alpert Medical School of Brown University and Rhode Island Hospital, Providence, RI

Methodology

- 3D models of the RCB were generated
- Inertial coordinate systems (ICS) were computed
- Bone volumes and bounding box (BB) dimensions were calculated
- Multiple linear regression was performed to express RCB volume as a function of animal age and weight

  (Vol = int + Age*B1 + Weight*B2 + Age*Weight*B3)
- Linear regression formulas were applied to predict BB dimensions given a specified volume
- Statistical shape analysis was performed to generate a mean-shaped RCB (RCB_{SSM})
- RCB_{SSM} model was anisotropically scaled by the ratio of the predicted BB dimensions to the BB dimensions of the RCB_{SSM}
- Bland-Altman analysis was performed to compare the predicted RCB and CT-derived RCB

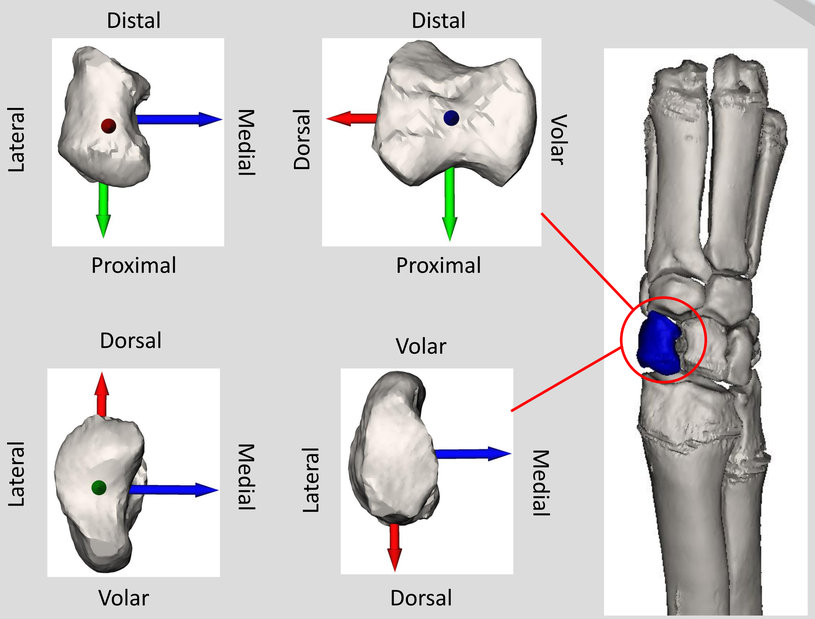

Fig 2. Right YMP specimen RCB with ICS in the dorsal (positive X; red), proximal (positive Y; green), and ulnar (positive Z; blue) directions.

Can Age and Weight Predict Radial Carpal Bone Size in a Porcine Preclinical Model?

Quianna M. Vaughan, Amy Morton, Douglas C. Moore, Joseph J. Crisco

Department of Orthopaedics, Warren Alpert Medical School of Brown University and Rhode Island Hospital, Providence, RI

Results

- Average volume of the RCBs= 1,808 mm^3
- Average BB dimensions
  - Volar-dorsal (VD)= 20.6 mm
  - Proximal-distal (PD)= 16.8 mm
  - Radial-ulnar (RU)= 11.9 mm
- Linear regression models demonstrated a high explanatory power for predicting BB dimensions from RCB volume (VD= 90%, PD= 73%, RU=51%)
- RCB_{SSM} volume= 1,756.5 mm^3
  - VD length = 20.1 mm,
  - PD length =15.8 mm
  - RU length of 11.4 mm
- Bland-Altman revealed a volumetric bias of -75.68 mm^3

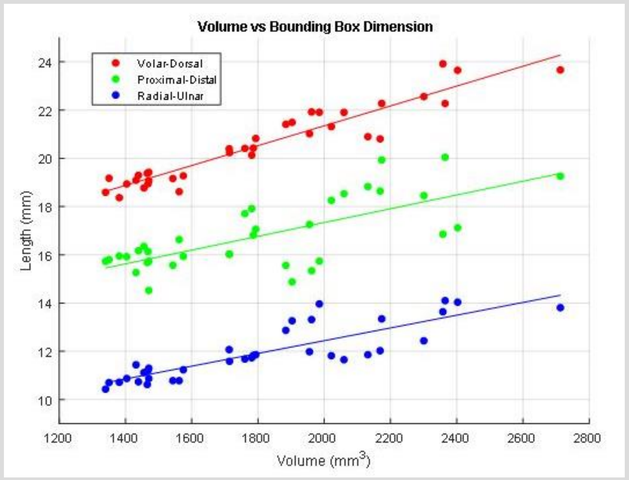

Fig 3. Regression analysis between RCB volume and each BB dimension (n=36).

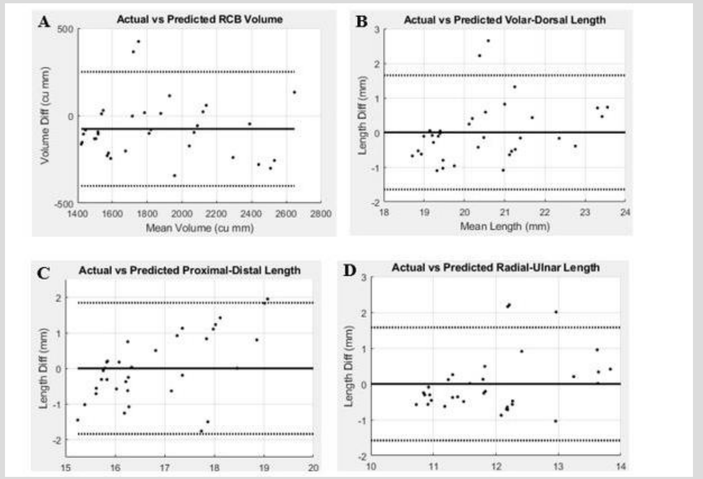

Fig 4. Bland-Altman analysis of RCB volume (A) and bounding box dimensions (B-D) between predictions from the model based on animal age and weight and measurements obtained from CT-generated bone models.

Can Age and Weight Predict Radial Carpal Bone Size in a Porcine Preclinical Model?

Quianna M. Vaughan, Amy Morton, Douglas C. Moore, Joseph J. Crisco

Department of Orthopaedics, Warren Alpert Medical School of Brown University and Rhode Island Hospital, Providence, RI

Conclusion

- Quantified the size of the RCB in the YMP
- Determined strong correlation between bone volume and animal age and weight, and between RCB volume and BB dimensions
- Scaling the RCB_{SSM} using our regression model outputs yield VD, PD, RU dimensions within 1% of the CT-generated RCBs
- Tendency to overestimate bone volume by 4.7%

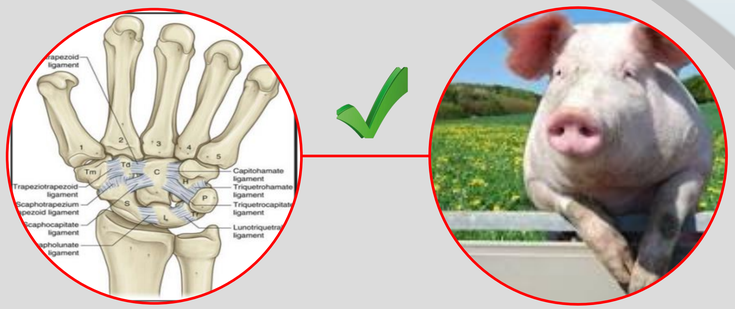

- A preclinical animal model for carpal bone replacement will provide a useful tool to advance novel treatments for wrist injury and degeneration

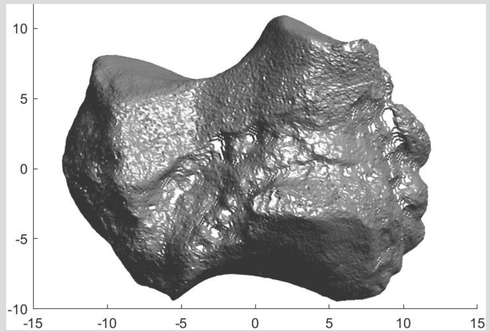

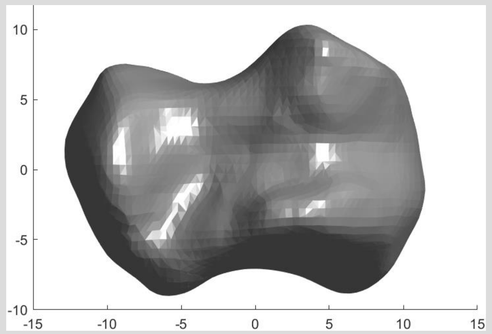

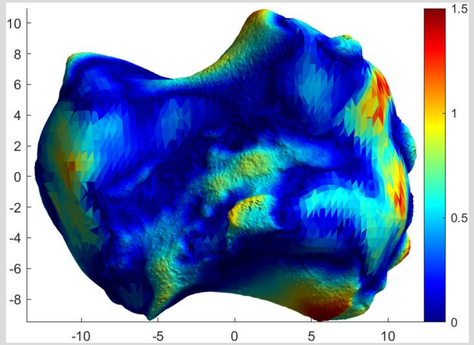

Sex Differences in Meniscal Cross-Sectional Area Profiles

Dominique A. Barnes1,2, Ata M. Kiapour3, Jillian E. Beveridge1,2, Mohammadreza Movahhedi3, Crystal J. Murray1,2, Martha M. Murray3, Braden C. Fleming1,2

1Brown University, Providence, RI, 2Rhode Island Hospital, Providence, RI, 3Boston Children's Hospital, Boston, MA

Introduction | Methods | Results | Discussion

The wedge-shape of the menisci is optimal for load transmission and shock absorption [1]

Meniscal injuries can impair the distribution of weight potentially leading to knee OA

Primary Goal

Compare the cross-sectional area (CSA) profile of the medial and lateral menisci between male and female subjects using statistical parametric mapping

Hypothesis:

The CSA profile of the medial and lateral menisci in females will be small than in males, even when normalized by knee size

Female patients have a 20% increased risk of having knee OA 5-years post surgery compared to males [2]

Morphological differences between the sexes may contribute to the higher risk of knee OA in females

[1] Menghini, D., et al. 2023. JOR
[2] Bodkin, S.G, et al. 2020. KSSTA

Interactive!
Click on any of these bubbles *to jump* to each section

Sex Differences in Meniscal Cross-Sectional Area Profiles

Methods

- 113 patients who underwent ACL surgery (70 females, median age 17.6)
- Constructive Interference in Steady State (CISS) MR images were collected at 6 months
- Medial and lateral menisci were automatically segmented from MRI
- Custom MATLAB script was written to measure the CSA of menisci over 60 equally spaced regions (Figure 1) from anterior root to posterior root (Figure 2)
- The CSA were normalized to the mediolateral bicondylar width (BCW) of the knee to account for differences in knee size (Figure 3)

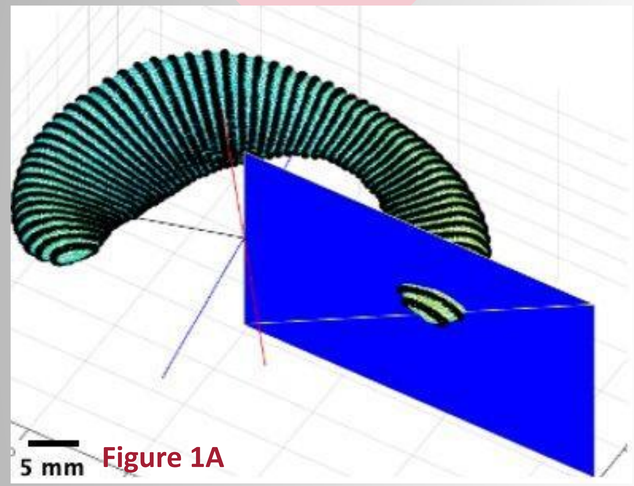

Figure 1A

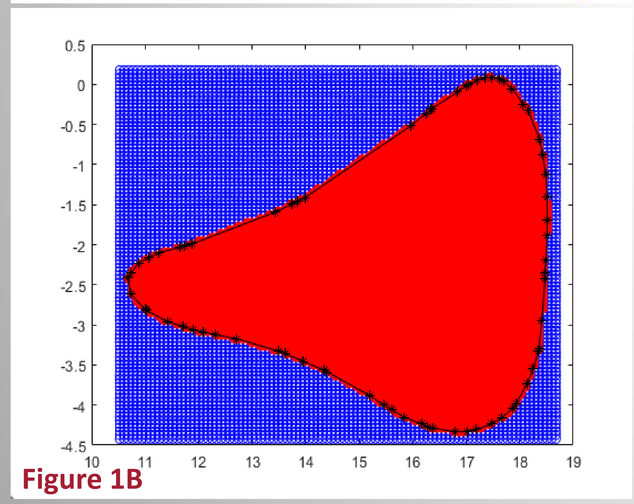

Figure 1B

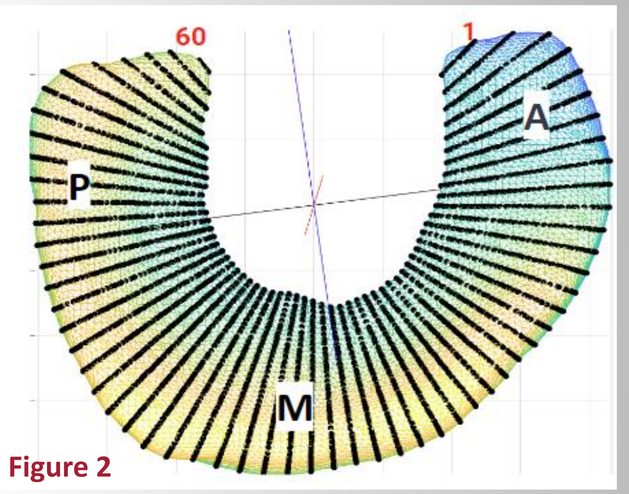

Figure 2

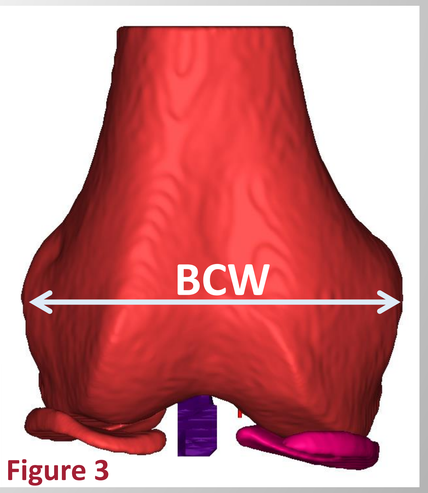

Figure 3

Interactive!
Click on any of these bubbles *to jump* to each section

Sex Differences in Meniscal Cross-Sectional Area Profiles

Introduction | Methods | Results | Discussion

Surgical Limb

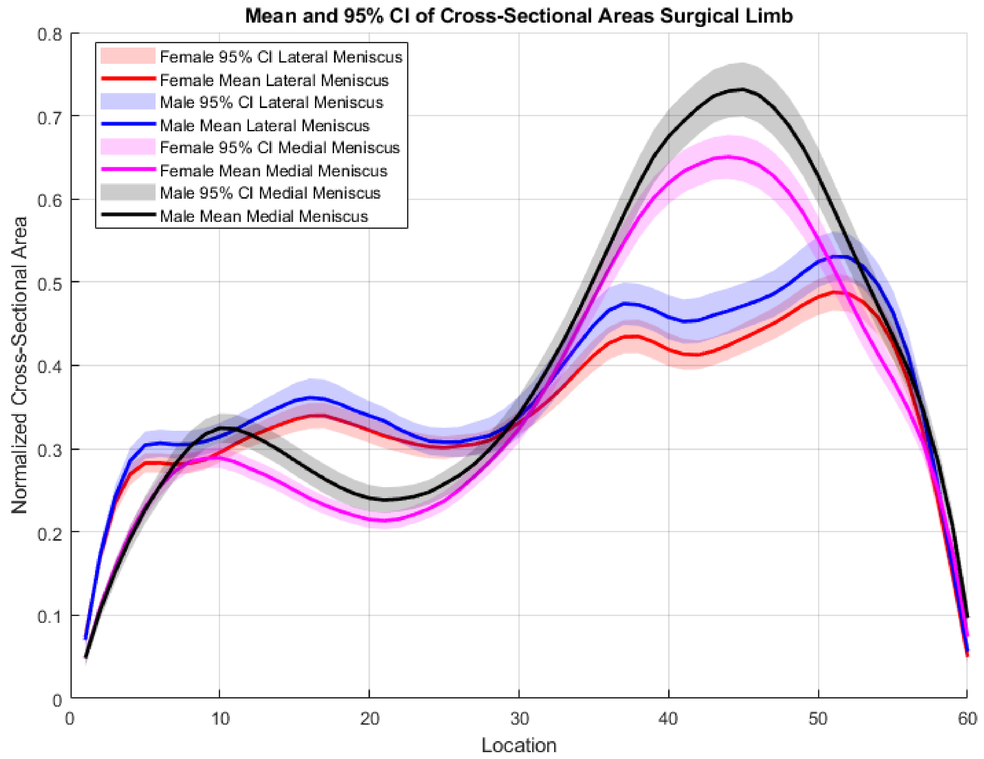

Non-Surgical Limb

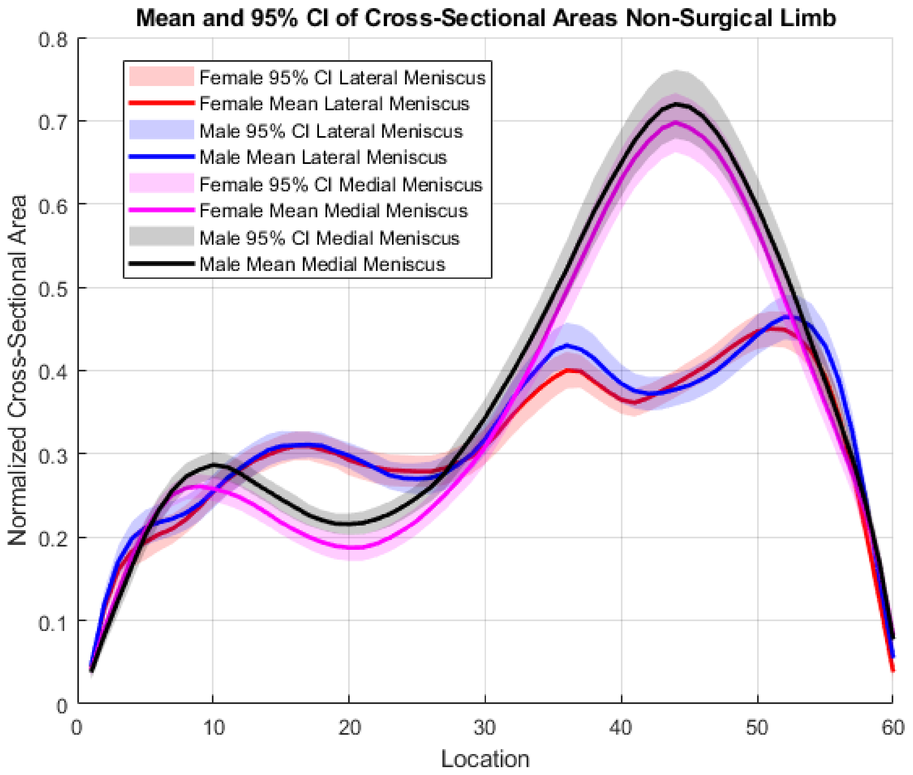

Interactive!
Click on any of these bubbles *to jump* to each section

Sex Differences in Meniscal Cross-Sectional Area Profiles

Surgical Limb

Non-Surgical Limb

Lateral Meniscus

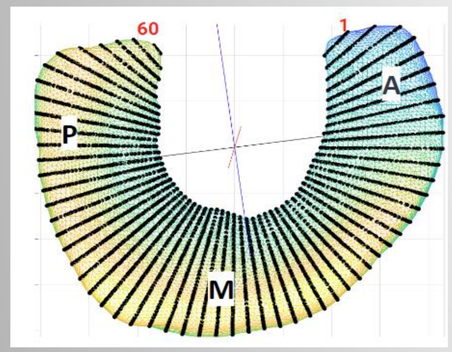

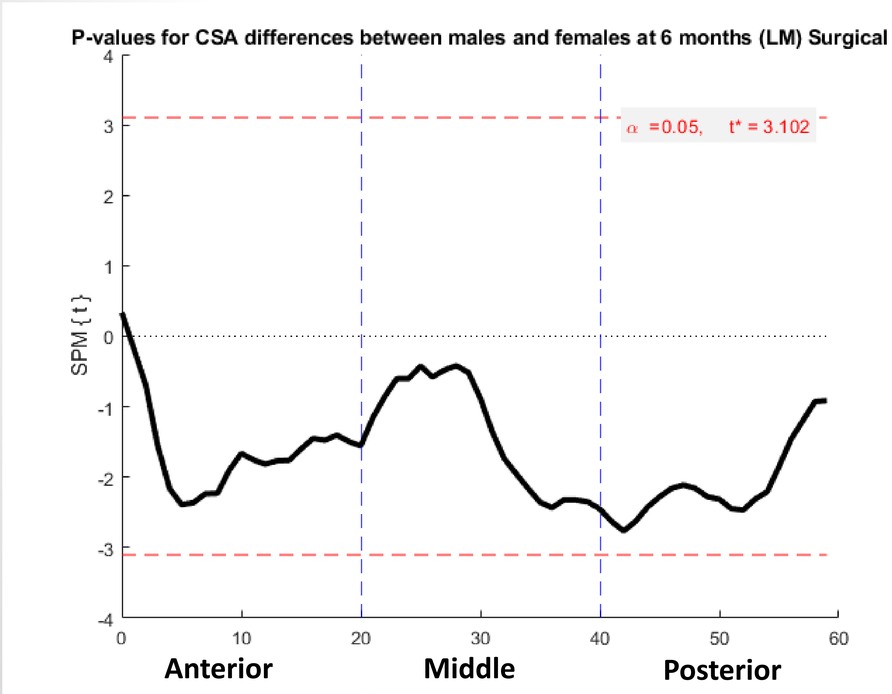

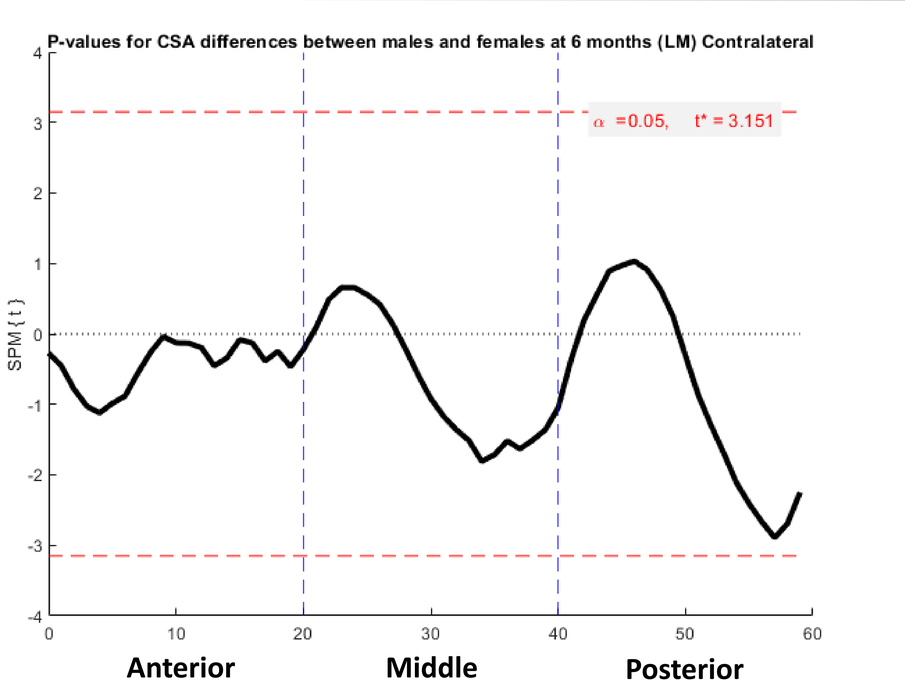

Interactive!
Click on any of these bubbles *to jump* to each section

Sex Differences in Meniscal Cross-Sectional Area Profiles

Surgical Limb

Non-Surgical Limb

Medial Meniscus

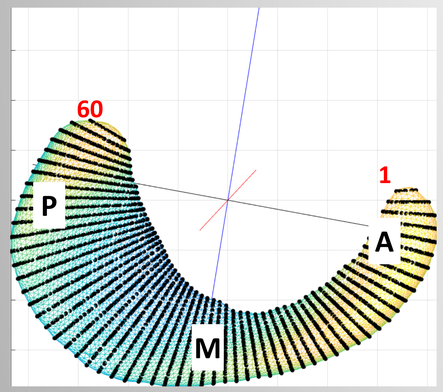

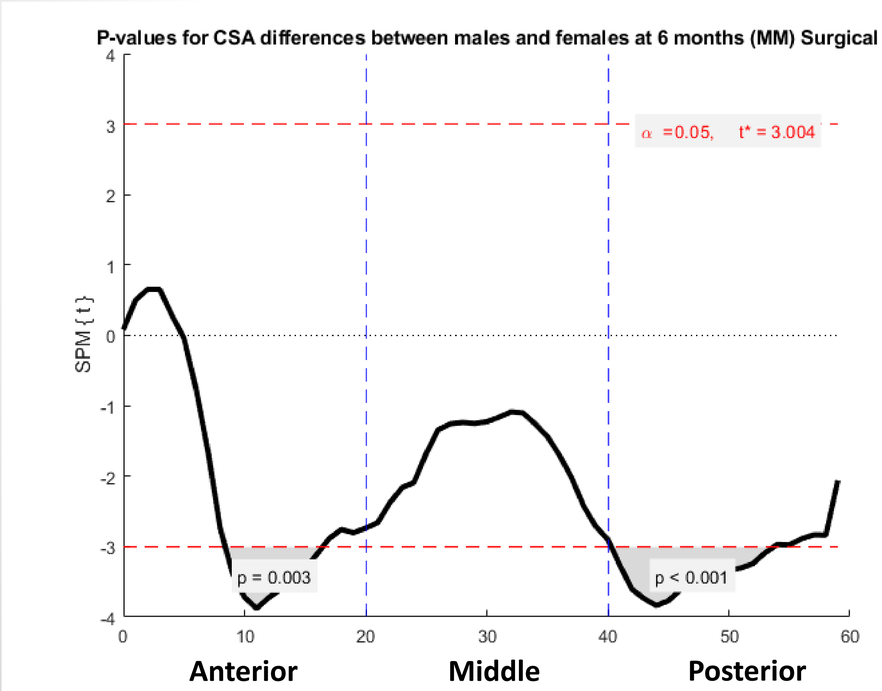

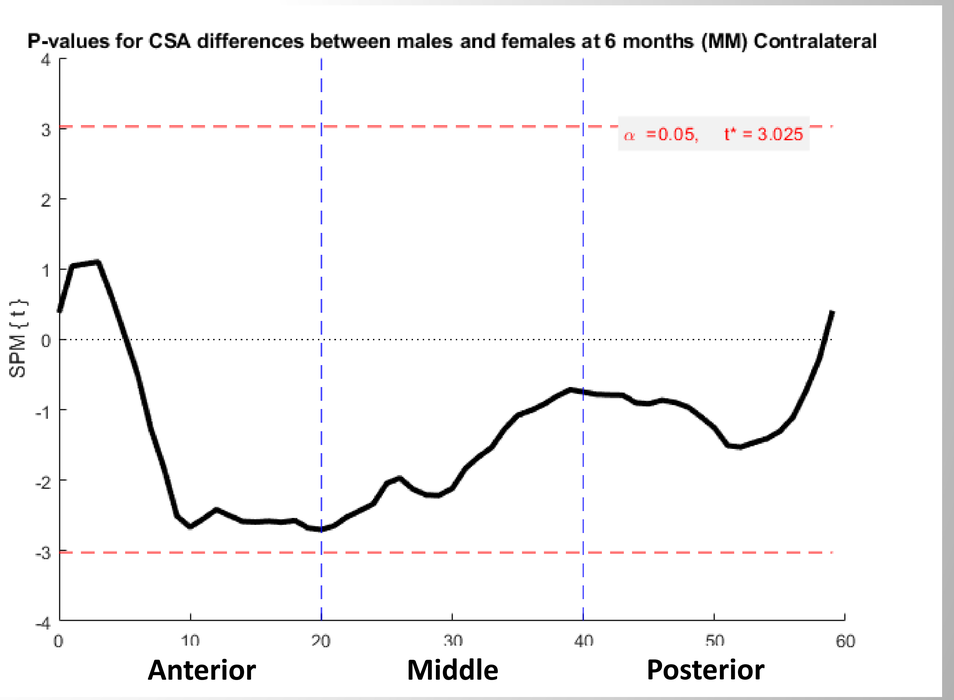

Interactive!
Click on any of these bubbles *to jump* to each section

Sex Differences in Meniscal Cross-Sectional Area Profiles

Discussion

- The knee surface area of females is 29% smaller than that of males even when matching for height and weight [3]
- Females that have undergone ACL surgery have a 20% increased risk of obtaining signs of knee OA within 5 years post-surgery compared to males [2]
- The significant differences observed in the medial meniscus of the surgical limb may be attributed to morphological changes following ACL surgery
- Identifying specific regions of the meniscus that undergo changes after surgery, particularly in female patients may inform the development of targeted rehabilitation strategies aimed at reducing post-surgical osteoarthritis

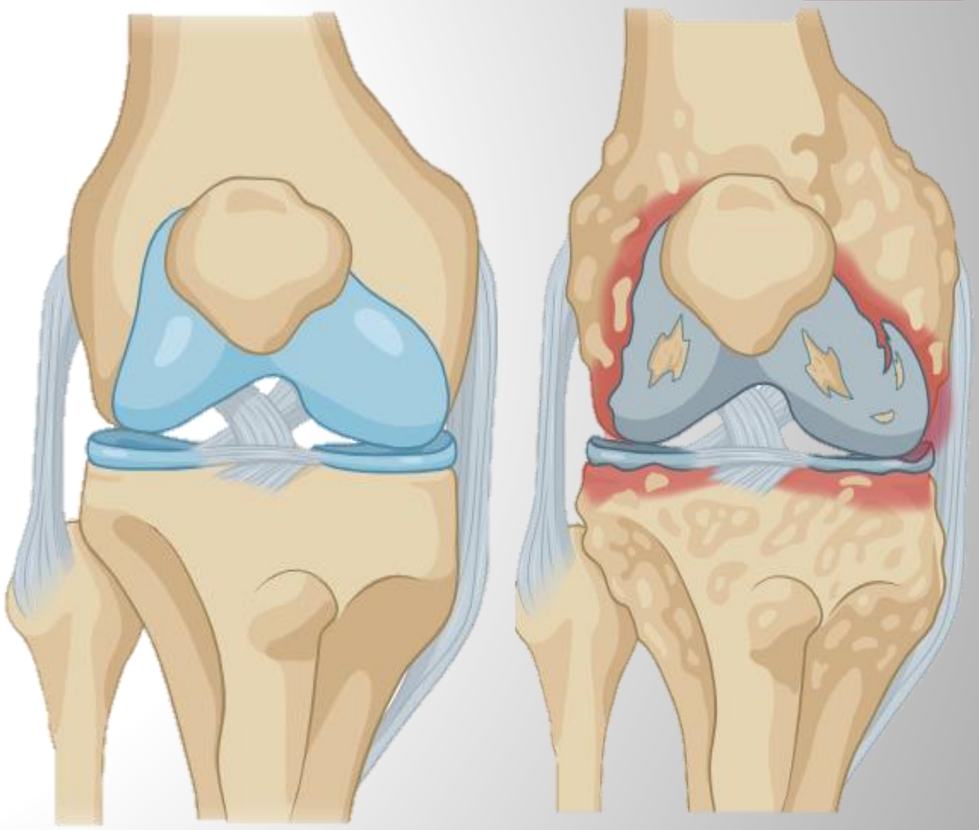

[2] Bodkin, S.G, et al. 2020. KSSTA
[3] Eckstein, Felix, et al. 2024 OARS
Images: BioRender

DESIGNING AN IMPLANTABLE TRAPEZIUM REPLACEMENT BONE FOR MEASURING *IN VIVO* LOADS AT THE BASE OF THE THUMB

J. J. Trey Crisco, Julia A. Henke, Daniel McDermott, Rohit Badida, Amy M. Morton, Josephine M. Kalshoven, Douglas C. Moore
Department of Orthopaedics

Rhode Island Hospital
BROWNHealth UNIVERSITY

ABSTRACT

The thumb is a common site for trauma and repetitive workplace injury, often leading to the development of osteoarthritis, with altered joint loading a primary mechanism for these pathologies. However, the *in vivo* loads at the joints are not known. The aim for this project was to design and assess the feasibility of an instrumented replacement trapezium capable of measuring loads *in vivo*.

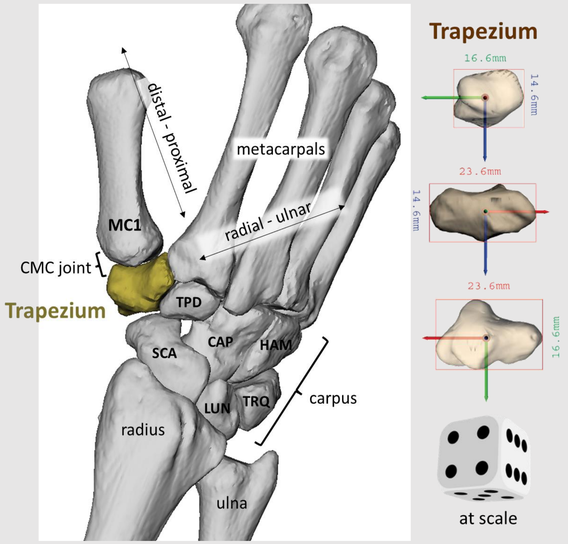

Fig. 1. CT derived anatomy of the wrist and trapezium carpal bone (left) and average bounding box dimensions (right).

METHODS

- Two sensor designs were evaluated: Tube and Diaphragm (Fig 2.)
- Tube: 9 strain gauges (120 Ω, VPG Sensors)
- Diaphragm: 5 strain gauges (1000 Ω, VPG Sensors)
- Calibration Testing
  - Gold Standard: 6 DOF load cell (Resolution: 0.25 N and 0.005 Nm. SI 580-20, ATI, Apex, NC)
  - The range of applied loads to Tube and Diaphragm designs were respectively:
    - Fx: -32.2 to 16.6 and -33.9 to 31.2
    - Fy: -125.2 to 0.2 and -68.5 to 0.1 (N)
    - Fz: -13.9 to 1.9 and -33.5 to 19.9 (N)
    - Mx: -0.5 to 0.5 and -0.11 to 0.17 (N)
    - My: -0.2 to 0.2 and -0.02 to 0.02 (Nm)
    - Mz: -0.3 to 0.5 and -0.15 to -0.11 (Nm)
  - Least Squares (Mat) and Supervised neural network (Deep) with two cascade-forward nets (Levenberg-Marquardt and Bayesian Regularization training functions for forces and moments, respectively), 70/30 train/test and 10k-fold validation on 68,037 data points. Strain gage failure was modeled by gage data removal.
  - Loading along the longitudinal axis of the first metacarpal (Fy) was set as the most critical outcome measure (x: volar, z: radial).
  - Accuracy was defined as the 95% CI of the limits of agreement (LOA) referenced to the 6 DOF load cell using a Bland-Altman analysis.

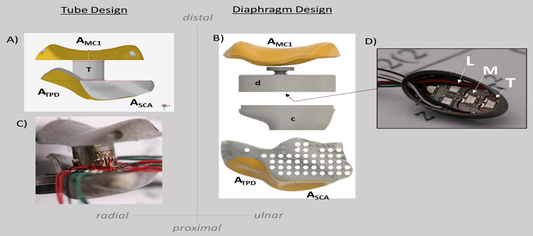

Fig. 2. The initial Tube (A & C) and Diaphragm (B & D) designs. The Tube design is based upon the approach previously developed for the knee, hip and shoulder, with gages on a central post (C). The Diaphragm design has strain gages on the underside of a flat, flexible membrane (D). Here, we report data from the left, middle and top strain gauges (L, M, T). Both designs incorporate polished surfaces for articulation with the MC1 (A_{MC1}), scaphoid (A_{SCA}) and trapezoid (A_{TPD}).

RESULTS

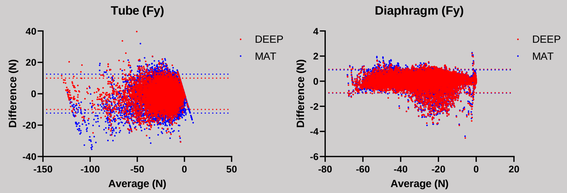

Fig. 3. Bland-Altman plots for Tube(A) and Diaphragm (B) designs for the most crucial load component Fy. R^2 for the MAT and DEEP algorithms for the Tube and diaphragm designs were 0.05, 0.03, 0.002, and 0.002, respectively. The dotted lines depict the LOA for each computational method within each design.

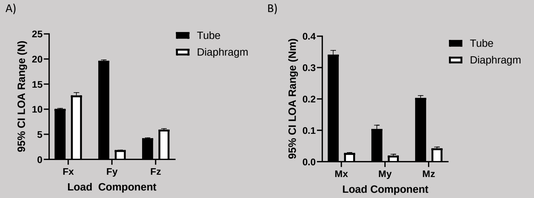

Fig. 4. Accuracy of the Tube and Diaphragm designs for forces (A) and moments (B) as assessed by the 95% CI of the LOA.

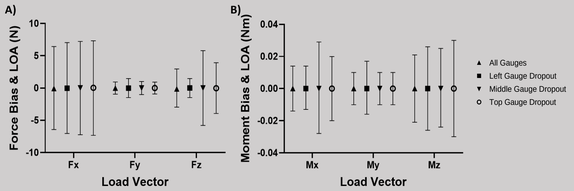

Fig. 5. Simulated single gauge failure in Diaphragm design for forces (A) and moments (B). "All" refers to all working gauges. Left Gauge Dropout, Middle Gauge Dropout, and Top Gauge Dropout refer to the simulated failed gauges depicted in Fig 2.

DISCUSSION & CONCLUSIONS

There were no notable differences in performance of the Tube and Diaphragm designs. While the tube design has been used successfully in knee, hip and shoulder implants, the small size of the trapezium bone, makes encapsulation of the electronics extremely challenging.

Additionally, a trapezium implant can only be secured via soft tissue fixation, as opposed to bone fixation in those larger joints. The Diaphragm design solves this problem. Thus, we are moving ahead with the diaphragm design instrumented with 5 strain gauge, with the goal of measuring loads across the thumb carpometacarpal joint *in vivo*, given its ability to measure axial loads with a 95% CI LOA of approximately 2 N. Many challenges remain before the device can be considered for FDA clearance and implantation in the humans. To minimize subject risk, the device will not be provided with a battery. The power and data systems (BLE) are being developed and evaluated first in benchtop testing, followed by the miniaturization and installation of the components within the diaphragm on a flexible circuit board. Mechanical components (fabricated from titanium (Ti6Al4V) will be welded and hermetically sealed, followed by fatigue testing for structural integrity.

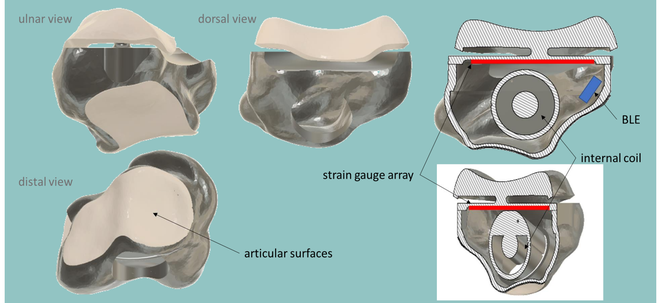

Fig. 5. CAD renderings of the current design. The articular surfaces will be polished and hardened with ion implantation. Power will be delivered inductively, via an external coil embedded in a glove. Load and temperature data will be transferred via Bluetooth Low Energy (BLE).

SIGNIFICANCE

An instrumented trapezium capable of measuring loads at the base of the thumb will be immensely valuable to clinicians, researchers, and implant designers who need accurate load data to understand the role of joint loading in thumb pathophysiology, to refine musculoskeletal models, to standardize pre-clinical testing for devices seeking FDA clearance, and to develop more effective and cost-effective surgical treatments.

ACKNOWLEDGEMENTS

This research was funded in part by NIH/NIAMS R21AR077201.

Challenges in Biomechanical Testing of the Rat ACL

John Holtgrewe[1], Samantha Zalk[1], Crystal Murray[1], Li Yue[1], Brett D. Owens[1], Jillian E. Beveridge[1]

[1]Brown University and Rhode Island Hospital, Providence, RI

Background and Aim

- Adolescent females experience anterior cruciate ligament (ACL) tears more frequently than males[1]
- Because the hormone relaxin-2 reduces collagen tensile stiffness,[2] its possible effects on the biomechanical properties on the ACL in a rat model of elevated relaxin-2 is of interest
- Using a fixture design previously described by others,[3] our preliminary work demonstrated that the reproducibility of rat ACL biomechanical properties was poor, characterized by unexpected large (>10%) bilateral asymmetries in tensile failure values[4]

Aim: **R**efine the approach used to quantify the biomechanical properties of the rat ACL such that bilateral asymmetry in biomechanical outcomes was no greater than 10%**.**

Methods

- Iterative process undertaken to refine fixture design testing showed high levels of bilateral asymmetry in ACL biomechanical properties

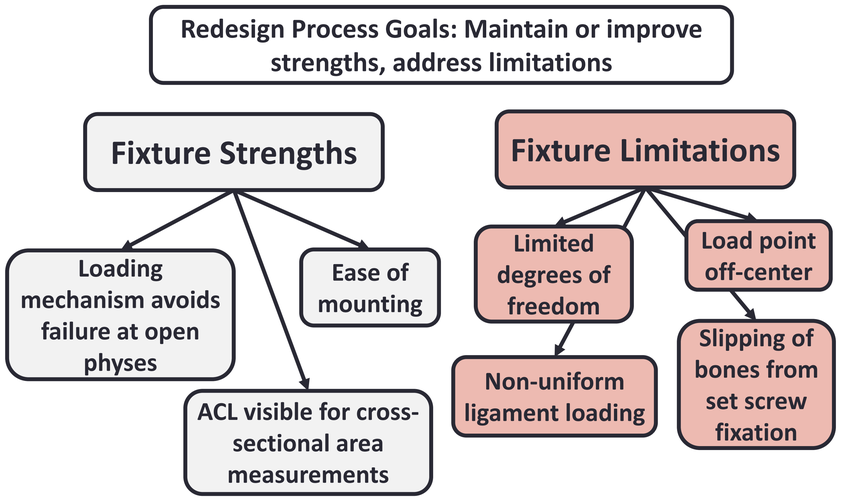

- Redesigned fixturing to address limitations through literature review and physical testing

Methods and Results

Ligament Loading

- Applying load at peak ACL extension, which is around 30º for quadrupeds, may lead to more uniformly loading the ligament[5]

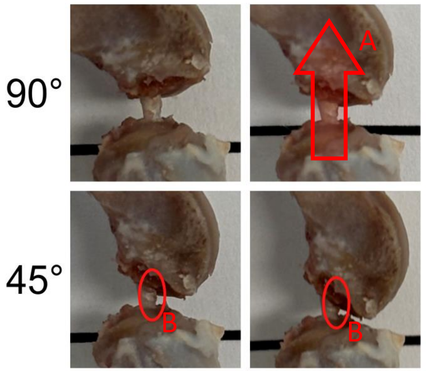

A. Direction of load applied to ACL
B. Visible wrinkling on anterior side of ACL at 45º and 30º flexion

60º flexion selected:
- *Near peak extension*
- *Uniform loading*

Figure 1. Rat knee at 4 flexion angles to investigate uniformity of ligament loading

Specimen Alignment

- Redesigned fixture to accommodate change in flexion angle and improve reproducibility of specimen alignment
- Eliminate moment arm induced by off-center load point in original design

A. Maintained features from initial design that support the open physis
B. Channel feature to reproducibly center femur in fixture
C. Centered load point

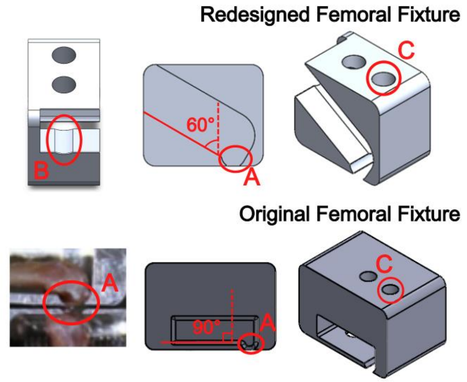

Figure 2. 3D models of redesigned and original femoral fixtures

Methods and Results cont.

Specimen Fixation

- Adapted method used in previous study to pot pig bones to pot rat bones in 9mm straws to provide larger and more unform shape for set screws to grip[5]

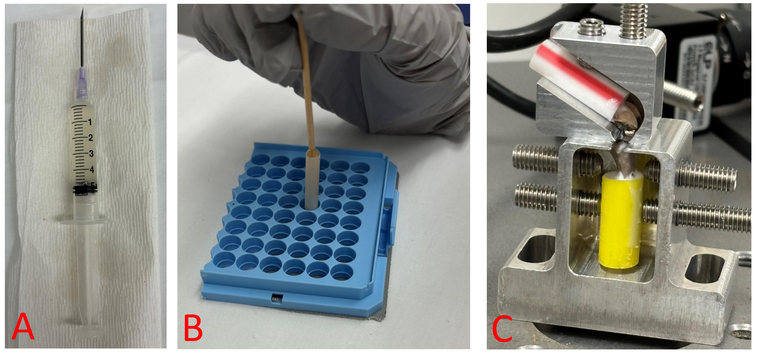

Figure 3. Potting method adapted for rat femur and tibia: A. 5ml syringe with casting resin (Smooth-Cast) B. Practicing placing bone in resin filled straw with applicator C. Potted femur and tibia placed in redesigned fixture setup

Discussion and Conclusions

- Achieving bilateral symmetry in measured rat ACL biomechanical properties continues to be a challenge
- Revisions were made to the testing setup to address limitations identified in first round of pilot testing
- Reduced degrees of freedom remain a design limitation
- The effectiveness of the testing modifications will be evaluated in additional testing as a next step

Acknowledgements & References

This project was supported by the Rhode Island Hospital Department of Orthopaedics.

1. Prodromos, CC. et al. Athroscopy (23), 2007. 2. Konopka, JA. et al. Am J Sports Med (48), 2019. 3. Konopka, J. et al. American J. Sports Medicine (48), 2020. 4. Yiannakopoulos, CK. et al. J Muskuloskelet Neuronal Interact (5), 2005. 5. Fleming, BC. et al. Am J Sports Med (37), 2010.

Muscle Activity Patterns During a Single-Leg Hop Landing in Healthy Males and Females

Crystal J. Murray,[1,2] Janine Molino,[1,2] John D. Holtgrewe,[1,2] Dominique A. Barnes,[1,2] Payam Zandiyeh,[3] Braden C. Fleming,[1,2] Jillian E. Beveridge[1,2]
[1]Rhode Island Hospital, Providence, RI; [2]Warren Alpert Medical School of Brown University, Providence, RI; [3]University of Texas Health, Houston, TX

Introduction

Anterior cruciate ligament (ACL) injuries occur 2-8 times more often in females,[1] though sex-specific risk factors explaining this elevated risk have yet to be fully described.[2] The objective was to apply a wavelet frequency analysis approach[3] to quantify muscle activity patterns from electromyography (EMG) signals during a 1-leg hop for distance.

Based on existing knowledge,[4,5] we hypothesized that females would have:

1) Greater quadriceps activity
2) Earlier hamstring activation
3) Larger Quadriceps:Hamstrings (Q:H) activation intensity ratios

Methods

Subjects: 12 females (30.5 ± 10 years) and 8 males (35.5 ± 6 years) with no history of knee injury were enrolled in this IRB-approved study.

Data: Surface EMG signals from quadriceps and hamstrings that were temporally synchronized with an 8-camera motion capture system and a force platform were recorded.

Analysis: A wavelet analysis approach,[3] was used to quantify muscle activity patterns based on EMG signal frequency, intensity, and timing *(Figure 1).* EMG amplitude was normalized to remove baseline participant differences. EMG time was normalized across three hop phases *(Figure 2).*
Three metrics were assessed: **[Metric 1]** Average median signal intensity; **[Metric 2]** Signal intensity profile: sum of the wavelet intensities at each time point during the hop; **[Metric 3]** Q:H ratio: median signal intensity of agonist/antagonist muscle pair.

Statistics: Generalized estimation equations and statistical parametric mapping (SPM).

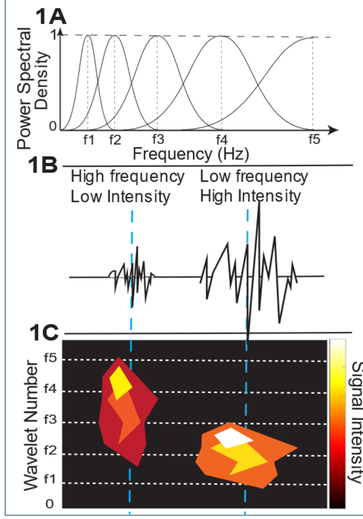

Figure 1 (left). *For each normalized time frame (x-axis), the corresponding frequency and amplitude of the signal (1B) can be visualized as a wavelet contour plot (1C). Darker colors represent lower signal amplitude/intensity. Placement of the wavelet contour along the y-axis is dictated by signal frequency (as developed in figure 1A).*

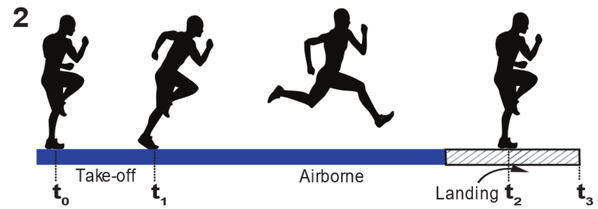

Figure 2 (above). *1-leg hop for distance hop phases. Take-off spans time(t) t_0 - t_1; Airborne = t_1 - t_2; Landing = t_2 - t_3. Hop phases were identified based on a priori biomechanical parameters.[3]*

Results

There were no statistically significant sex differences in any of the wavelet muscle activation metrics evaluated.

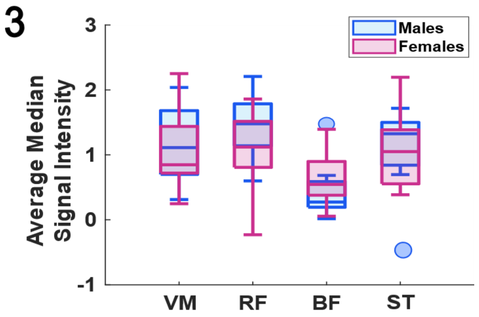

Figure 3. [Metric 1] *Average median signal intensity of males and females for quadriceps (VM-vastus medialis & RF-rectus femoris) and hamstrings (BF-biceps femoris & ST-semitendinosus) during the airborne phase.*

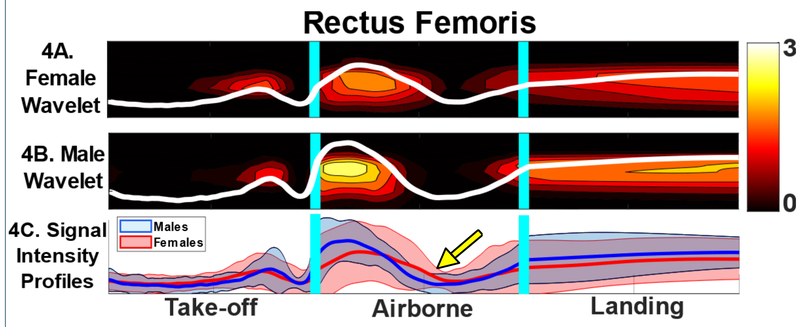

Figure 4. [Metric 2] *4A & 4B are EMG wavelet contour plots of the rectus femoris muscle for each sex. The white line is the signal intensity profile [Metric 2], overlayed on the wavelet contour plot, secondary y-axis is total signal intensity. 4C compares the signal intensity profiles between sexes. The shaded region corresponds to the 95% CI. Yellow arrow indicates a timepoint where the difference approached significance (p=0.057) following SPM analysis.*

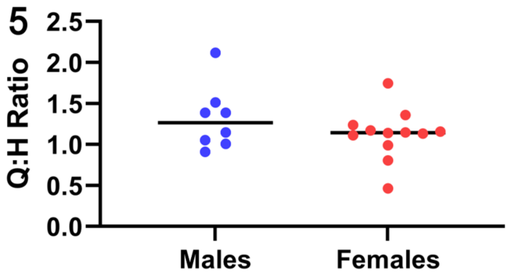

Figure 5. [Metric 3] *(Q:H) median signal intensity ratios for males and females during the airborne phase.*

Discussion

Despite implementing a more sensitive approach, our analysis did not reveal sex differences in the neuromuscular patterns assessed.

- Contrary to previous reports,[4] there were no sex-specific differences in median quadriceps and hamstring intensity or Q:H ratios in the present study; however, the temporal analysis of the signal intensity profile suggests nuanced sex-specific differences in muscle activation timing.
- Females tended to exhibit prolonged quadricep muscle activation during the airborne phase of the hop. Evidence from a multi-modal modeling approach of a similar hop activity suggests that greater quadriceps force induces ACL strain.[6] If true, this paradigm of prolonged quadriceps activity without concurrent hamstring activity could be implicated in a higher-risk neuromuscular landing strategy in females.

A larger sample size and applying more sophisticated machine learning approaches may provide additional insight and ability to resolve small, but meaningful sex-based differences in neuromuscular activity patterns. These avenues are currently being explored as part of an ongoing study examining kinematic and neuromuscular control in competing ACL surgeries.[3]

Significance/Clinical Relevance

This information provides a baseline to interpret sex differences that may arise with, or are amplified by, ACL injury and surgery.

References

[1] Sutton KM., et al. J Am Acad Orthop Surg. (2013); [2] Seyedahmadi M., et al. BMC Sports Sci Med Rehabil. (2022); [3] Zandiyeh P., et al. J Biomech. (2022); [4] Bencke J., et al. Front Physiol. (2018); [5] Coats-Thomas MS., et al. J Orthop Res. (2013); [6] Englander ZA., et al. Am J Sports Med. (2022)

Acknowledgements

NIH NIAMS (K99/R00-AR069004, R01-AR047910, R01-AR074973; R01-AR083168); NIGMS (P30-GM122732, P20-GM139664); and the Lucy Lippitt Endowment.